

Solvent Influences the Morphology and Mechanical Properties of Electrospun Poly(L-lactic acid) Scaffold for Tissue Engineering Applications

A.Sh. Asran,^{*1,2} M. Salama,^{2,3} C. Popescu,³ G.H. Michler¹

Summary: Electrospun micro- and nanofiber scaffolds have gained interest in biomedical applications, especially in tissue engineering, because they can be used to reproduce the structure of the extracellular matrix (ECM) of natural tissue. The selection of the solvent is an important factor which affects the diameter, the surface morphology and the crystallinity of the electrospun fibers, and, accordingly, their mechanical properties as well as their degradation kinetics. Furthermore, the surface morphology of the electrospun fibres can be controlled by solvent vapour pressure to produce porous structures which might be helpful for cell adhesion and proliferation. In the present work, poly (L-lactic acid) (PLLA) has been electrospun using solvents with different vapour pressures to investigate the influences of the solvent vapour pressure on morphology, diameter, crystallinity and mechanical properties of the electrospun fiber scaffolds. The results show that the vapour pressure of the solvents (or solvent mixtures) play an important role in the fiber diameter and crystallinity. Furthermore, the crystallinity of the fibers is increased by lowering the vapour pressure of the used solvent. In addition, the mechanical properties (e.g., tensile strength and Young's modulus) are strongly dependent on morphological features such average fibers diameter. The smaller the average diameter, the higher the tensile strength and Young's modulus.

Keywords: crystallinity; electrospinning; fibrous scaffold; mechanical properties; poly(L-lactide); solvent vapour pressure

Introduction

Bioresorbable synthetic polyesters are attractive materials in biomedical applications, since they offer a wide range of physical, chemical, and mechanical properties. Degradation rates can be better controlled than for natural bioresorbable polymers.^[1,2] Poly (lactic acid) (PLA), poly (glycolic acid) (PGA) and their copolymers are among the few synthetic polymers which have been shown to be biocompatible,

biodegradable, easy to process and consequently approved for human clinical uses. Furthermore, the main advantage of PLA and PGA is their degradation by simple hydrolysis of the ester backbone in aqueous environments such as body fluids. The degradation products are finally metabolized to carbon dioxide and water or excreted via the kidneys, so it is not necessary to remove the device from the implantation site after tissue healing.^[3] Vert et al. found that no significant amounts of PLLA degradation products accumulated in any of the vital organs,^[4] which makes it very convenient for devices with a temporary function. As a result, PLA has found numerous biomedical applications such as surgical sutures,^[5] materials for tissue repair and regeneration,^[6] bone tissue

¹ Institute of Physics, Martin Luther University Halle-Wittenberg, D-06099 Halle, Germany

E-mail: ashraf.abdel-sayed@physik.uni-halle.de

² National Research Centre, El Buhoth St, 12311 Cairo, Egypt

³ DWI an der RWTH Aachen, D-52056 Aachen, Germany

engineering,^[7] and carriers for drug and gene delivery.^[8]

Electrospinning technique has proven to be a relatively simple and versatile method for forming non-woven fibrous scaffolds with fiber diameters ranging from few nanometers to several micrometers, a size range that is otherwise difficult to access by conventional non-woven fiber fabrication techniques.^[9,10] The fibers are formed using an electrically driven charged jet of polymer solution (or polymer melt) emitted from the apex of a cone formed on the surface of a droplet of polymer solution. As this jet travels through the air, it solidifies leaving behind a polymer fiber to be collected on an electrically grounded target as a nonwoven fabric.^[11-14] The electrospun nano and/or micro fibers are investigated in view of various biomedical applications such as tissue engineering,^[15] wound dressing,^[16] and manufacture of artificial blood vessels^[17] since they mimic the structures properties of native extracellular matrix (ECM) of natural tissue^[18-20] and they possess a high surface area to volume ratio which may provide more appropriate substrates for cell attachment.^[21]

It is well known that the electrospinning technique depends on various processing parameters such as solution properties, and choice of the solvent which affect the solution properties, (e.g., viscosity, surface tension and conductivity) which in turn, influences the electrospinnability, surface morphology and diameter of the electrospun fibers.^[22-25] Recently, many researchers showed that surface morphology of the biomaterial scaffolds play a vital role in controlling cell adhesion, proliferation, shape, and function.^[26,27] Wannatong et al. investigated the effect of six solvents on morphology and size of the electrospun polystyrene fibers^[28] Although several papers reported the effect of processing variables on the fiber shape and distribution,^[29] to our knowledge there are no publications on the relation of solvent vapor pressure and morphology,

crystallinity and mechanical properties of the electrospun fibers.

Herein, our main objective is to manufacture non-woven PLLA scaffolds using various solvents with different vapor pressures and to study systematically the effect of the solvent system on morphology, diameters and crystallinity of the electrospun PLLA fibers. The fibers were characterized mainly by scanning electron microscopy (SEM), and thermal analyses (DSC, TGA and DTGA) have been used to study the crystallinity of the electrospun fibers and the mechanical properties of the resulting PLLA scaffolds.

Materials and Methods

Materials

PLLA (Cargill, $M_w = 200$ kg/mol) was purchased from Dow Chemical, Germany, and used without further treatment or purification. Chloroform (CHCl_3), Dichloromethane (DCM), and Ethanol (EtOH) were purchased from Carl Roth GmbH, Germany.

Electrospinning of PLLA

To obtain electrospinnable solutions, PLLA was dissolved in different solvents or solvent mixtures, as there are CHCl_3 , DCM, CHCl_3/DCM (50:50), $\text{CHCl}_3/\text{EtOH}$ (80:20), DCM/EtOH (80:20), to prepare 10 wt% solutions. These solutions were vigorously stirred using a magnetic stir bar for at least 24 h at room temperature to ensure homogeneity. Electrospinning was carried out at room temperature in a vertical spinning configuration, using a 1 mm inner diameter flat-end needle with a 15 cm working distance and a flow rate of 0.1 ml/h. The applied voltages were in the range of 3 to 20 kV, driven by a high voltage power supply (Heinzinger PNC 30000, Germany). The electrospun fibers were collected directly on a grounded metal grid, and the deposited nonwoven electrospun fibers were carefully peeled out for further investigations.

Scanning Electron Microscopy (SEM)

To image the morphology of the as-spun fibers by scanning electron microscopy

(JSM 6300, JEOL), the specimens were collected on glass slides and gold sputtered to 20 nm thickness for better conductivity during imaging. The diameters of the fibers and their size distributions were analyzed using image analysis software (AnalySIS, Soft Imaging System Co., Germany).

Differential Scanning Calorimetry (DSC) and Thermo gravimetric Analysis (TGA)

A NETZSCH DSC 204 with nitrogen as purge gas was used to investigate the crystallization behavior of PLLA scaffolds. About 5 mg of sample was sealed in aluminum pans, heated from 25 to 250 °C and kept at 250 °C for 2 min in order to eliminate the thermal history. Then the sample was cooled down with 10 K/min to the 25 °C, for complete crystallization of the matrix. The heat evolved during non-isothermal crystallization was recorded as a function of time. Then the specimens were heated again with 10 K/min to record the melting. The melting temperature was taken as the peak temperature of the fusion process. The DSC curve puts into evidence the glass-transition temperatures (T_g), the melting temperature (T_m) and allows calculating the crystallinity. The crystallinity (X_c) is estimated from the area of the endotherm by equation (1)

$$\%X_c = \Delta H_f / \Delta H_f^o \times 100 \quad (1)$$

Where ΔH_f is the measured enthalpy of fusion from DSC thermograms and ΔH_f^o is the enthalpy of fusion for 100% crystalline PLLA (93,6 J/g).^[30]

A NETZSCH TG 209C was used for gravimetric analysis (TGA) of PLLA scaffolds. About 5 mg of sample was weighted in Al_2O_3 pan and then heated from room temperature to 750 °C at a heating rate of 10 °C/min under a nitrogen flow. All the graphs were analysed by using the NETZSCH software.

Mechanical Properties

Mechanical properties of electrospun scaffolds were measured on a Dia-Stron MTT 675 miniature tensile tester (Dia-Stron Ltd.

Andover, UK) using a 10 N load cell under a constant tensile rate of 10 mm · min⁻¹ at 25 °C. All samples were cut into rectangle shapes with dimensions of 20 mm × 5 mm. At least seven samples were tested for each type of electrospun fibrous scaffold.

Results and Discussion

Effect of Solvent Vapour Pressure on Morphology and Diameters of the As-Spun PLLA Fibrous Scaffolds

In our present work, three solvents obtained to get five solutions with different vapor pressures have been used to dissolve PLLA for the solutions preparation. The vapor pressure of binary solution can be calculated according to Raoult's law, using the example of a solution of two liquids, A and B, the total vapor pressure (P_{tot}) for the solution is equal to the sum of the vapor pressures of the two components, (P_A) and (P_B) (See equation 2)^[31]

$$P_{tot} = (P_A)_{pure}X_A + (P_B)_{pure}X_B \quad (2)$$

The individual vapor pressure for each component is

$$P_{tot} = (P_A)_{pure}X_A \quad (3)$$

Where (P_A)_{pure} is the vapor pressure of the pure component and X_A is the mole fraction of the component in solution. 1

Figure 1 shows the influence of the selection of the pure solvent or the composition of solvent mixtures, respectively, on the surface morphology and diameter distribution of PLLA fibers. The micrographs indicate that the composition of the solvent and their vapour pressure

Table 1.
Vapor pressure of the solvent and mixture solvents.

Solvent	Vapor pressure at 20 °C [mmHg]
Dichloromethane (Solvent I)	350
DCM/EtOH (Solvent II)	288.7
DCM/CHCl ₃ (Solvent III)	253
Chloroform (Solvent IV)	156
CHCl ₃ /EtOH (Solvent V)	133.6

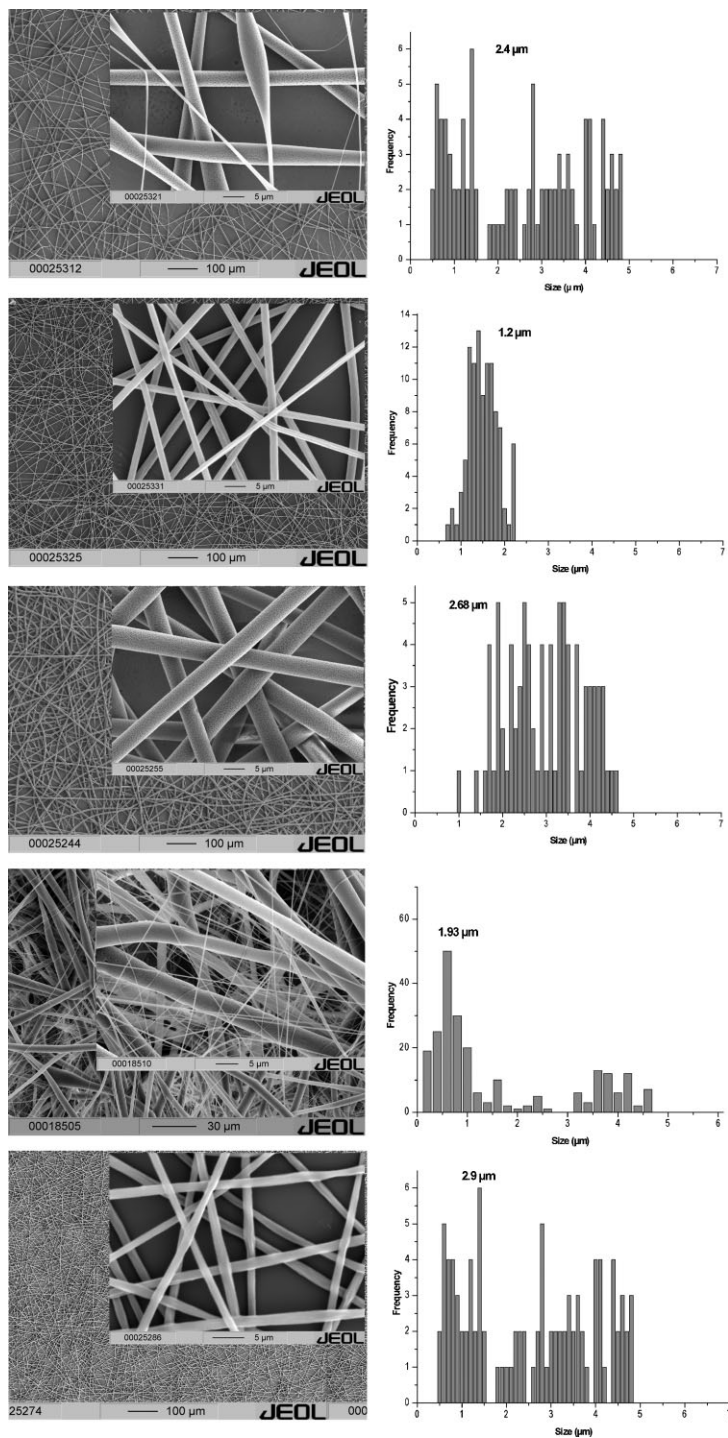


Figure 1.

Scanning electron micrographs for electrospun PLLA fibers and their diameter distributions using solvents with different vapor pressures. Fibers I, II, III, IV and V are the electrospun PLLA fibers using solvent I, II, III, IV and V, respectively.

cause significant changes of the fiber size distribution, shape and overall morphology due to the evaporation of the solvent and the variation of the viscosity.

It is observed that, using solvent I (high vapor pressure), one obtains a broad diameter distribution (420 nm–4.5 μm) of the fibers, which have a porous surface and a mean diameter of 2.4 μm . This porous morphology may support the exchange of gas and metabolites from the tissue and may favor a cell adhesion distributed throughout the biomedical device, allowing the formation of an organized network of the tissue constituents. In contrast to this result, no pores on the surface have been found when using solvent II. The fibers have a smooth surface morphology and a narrow diameter distribution (600 nm to 2.2 μm), with mean diameter of 1.2 μm . Using solvent III one obtains fibers with diameter distribution in the range of 870 nm to 4.7 μm , with a regular arrangement of surface pores and a mean fiber diameter of 2.65 μm . The number of surface pores is decreased when using solvent IV. The obtained fibers have diameters bigger than for the case of using the other solvents, and the diameter distribution is broad, ranging from 700 nm to 4.6 μm . The mean diameter is 1.93 μm . Solvent V produces uniform fibers

without pores but with a broad diameter distribution (400 nm–4.8 μm) and a mean diameter of 2.9 μm .

As it appears, the value of vapour pressure allows controlling the mean fibre diameter and the diameter distribution broadness. The vapour pressure affects also the surface morphology of PLLA scaffolds by inducing or stopping the formation of pores.

Thermal Analysis (DSC & TGA)

The glass transition temperature (T_g), crystallization temperature (T_c), melting temperature (T_m), and crystallinity (X_c) were determined from the second heating run. DSC thermograms are shown in Figure 2, and the numerical data are given in Table 2.

Like any semi crystalline polymer, PLLA has an amorphous phase, with randomly arranged macromolecules, and crystalline phase with a regular structure. When the polymer solution is electrospun, the jet ejects from the needle tip and polymer chains are stretched in the direction of the electrostatic field (along the fiber direction). The solvent starts evaporating within a very short time scale that generally leads to a lowering of the temperature (like quenching).^[32] The solidification process reduces the mobility of the macromole-

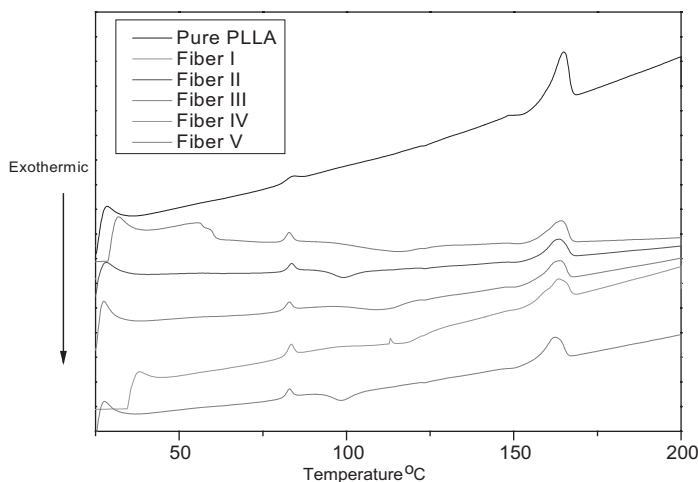


Figure 2.

DSC thermograms for electrospun PLLA fibrous scaffolds obtained by using different solvents.

Table 2.

DSC characteristics of PLLA scaffolds manufactured using different solutions.

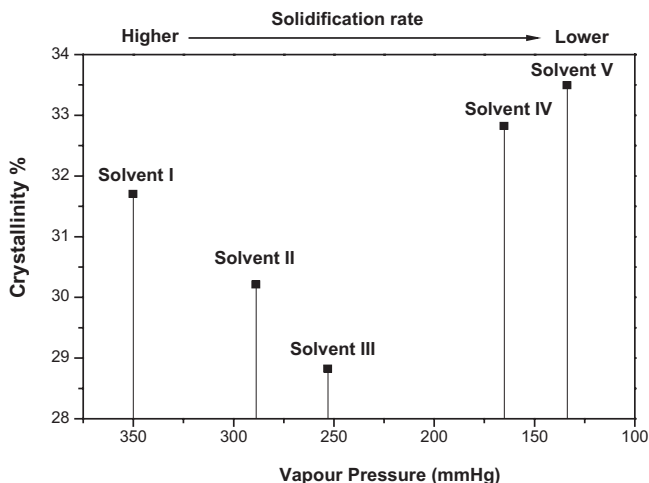
	T_g	T_m	T_c	ΔH_m	X_c
Bulk PLLA	80.7	164.8	–	31.6	33.7
Fiber I	56.5	158.4	118.5	29.7	31.7
Fiber II	56.7	158.1	120.2	28.3	30.2
Fiber III	55.4	158.4	121.8	27.0	28.8
Fiber IV	54.7	157.6	120.8	30.7	32.8
Fiber V	57.1	160.4	117.6	31.3	33.5

cules, and the degree of crystallinity of the electrospun fibers is lower than that of the initial bulk materials (see Table 2). In addition, one also observes the decrease of the glass transition temperature (T_g) of the electrospun fibers. Furthermore, it is noticeable that the melting temperature for the spun PLLA fibrous scaffolds does not change significantly, which indicates that the solvent vapor pressure does not influence it.

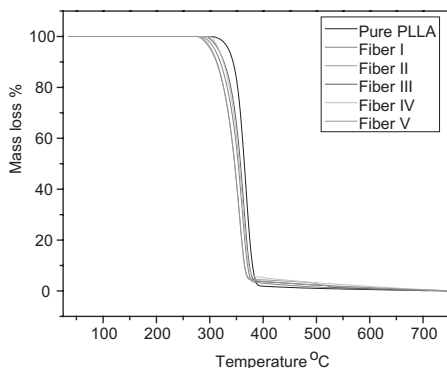
When using a solvent with high vapor pressure (solvent I), the time for the crystal growth is not sufficient, and the electrospun fibers will exhibit a crystallinity lower than in the bulk material. In case of using solvent (I), the crystallinity of the PLLA fibers is 31.7%, compared to a crystallinity of 33.7% for bulk PLLA. In addition, using solvents with lower vapor pressure (solvent II and III), the rate of jet solidification is

decreased and thereby the evaporation of the solvent occurs during the arrangement of macromolecules. Thus, the development of more perfect crystalline structures is hindered. As a consequence, fibers II and III exhibit degree of crystallinity of 30.2% and 28.8%, respectively. On the contrary, solvents with a slower evaporation rate (solvent IV and V), give more time for the crystals rearrangement and facilitate the development of a highly crystalline structure. As a result, the electrospun fibers IV and V exhibit crystallinities of 32.8% and 33.5%, respectively (see Figure 2). The previous results indicate that the choice of the solvent with a suitable vapor pressure is an important issue which will affect the crystallinity of the electrospun nanofibers. H. Tsuji et al. have studied the effects of annealing on the thermal properties, morphologies and mechanical properties of poly(L-lactide) (PLLA) and they evaporated the solvent rapidly to avoid formation of a highly ordered structure.^[33]

TGA and first derivatives of TGA (DTGA) for electrospun PLLA with different solvents (Figures 4 and 5) showed that all samples exhibited a distinct weight loss stage at 283–390 °C (wt % loss of ~98%), corresponding to the pyrolysis of the PLLA chains. The temperature of the

**Figure 3.**

Effect of the solvent vapor pressure of the solutions on the crystallinity of spun PLLA scaffolds.

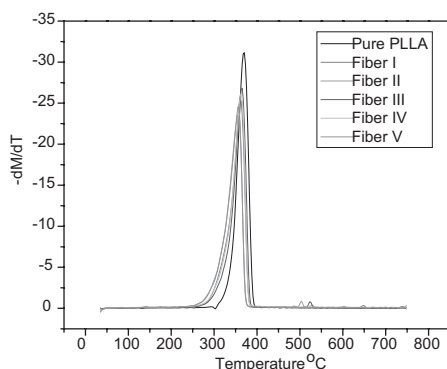
**Figure 4.**

TGA of PLLA scaffolds by using different solutions.

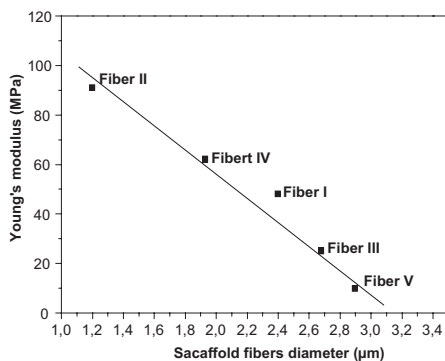
maximum mass loss rate is $\sim 369^{\circ}\text{C}$ for the bulk PLLA and $\sim 362^{\circ}\text{C}$ for the electrospun fibers of PLLA using different solvents, which may be due to shorter chains in case of the fibers. Since the thermal decomposition range of all electrospun fibers of PLLA is almost the same, we assume that the solvent vapor pressure has no significant influence on thermal properties of the electrospun PLLA.

Mechanical Properties (Young's Modulus and Tensile Strength)

Mechanical properties of the electrospun PLLA scaffold with different solution were discovered. Values of Young's modulus and tensile strength are plotted against the average fiber diameter for the electrospun PLLA scaffolds using different solvents (Figures 6 and 7). The results showed that

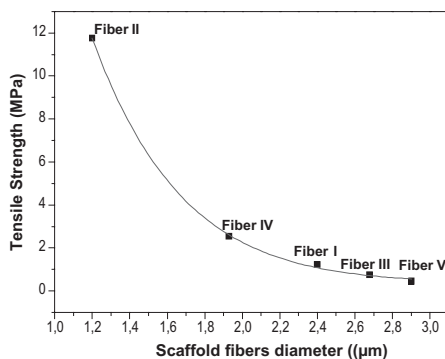
**Figure 5.**

DTGA of PLLA scaffolds by using different solutions.

**Figure 6.**

Effect of average fiber diameters on the Young's modulus (MPa).

Young's modulus and tensile strength of the as-spun fiber scaffolds decrease markedly by increasing the average fiber diameters, which can be attributed to the better molecular orientation in smaller nanofibers. Similar results are discussed independently by Wong et al.^[34] This leads to the conclusion that Young's modulus and tensile strength of the as-spun fibers are relatively dependent of the solvent vapor pressure, which has a great effect on the final morphology and diameter of the electrospun fibers. According to Arinstein and Zussman, the relaxation process which is generated by the evaporation of solvent within electrospun fibers, can significantly affect the mechanical properties of polymeric nanofibers.^[35]

**Figure 7.**

Effect of average fiber diameters on the tensile strength (MPa).

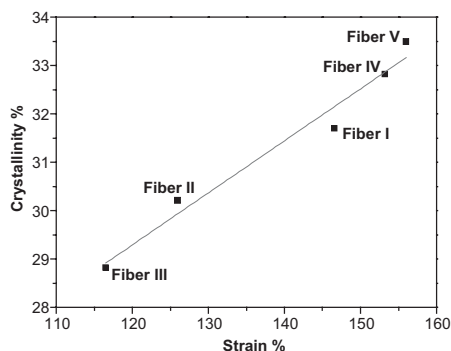


Figure 8.
Effect of fiber crystallinity on the break strain %.

Since the mechanical properties of electrospun fibers are closely related to crystalline morphology and molecular orientation, the increase in crystalline morphology and its orientation are other important issues. In other words, higher the crystallinity is, higher the fiber modulus. Furthermore, the crystallinity of the as spun fibers is influenced by the rate of evaporation of the solvent during the electrospinning jet reaches the collector. Thus, the electrospun PLLA fibrous scaffolds that are produced from polymer solutions using solvent with lower evaporation rate have higher degree of molecular orientation and crystallinity, and consequently a larger strain at break, as shown in Figure 8.

Conclusion

In this work, we have investigated the effects of solvent vapour pressure on the morphology, diameters, crystallinity and mechanical properties of electrospun PLLA fiber scaffolds. The results indicate that the mechanical properties, discussed in terms of tensile strength and Young's modulus, are strongly dependent on morphological features such average fibers diameter. The lower the diameters average the higher the tensile strength and young's modulus. It has been revealed that the vapour pressure of the solvent is a vital

factor which affects the fiber morphology (the degree of the crystallinity), diameter and consequently influences also the mechanical properties. Solvents with a low evaporation rate (low vapor pressure) allow enough time for the crystals formation and facilitate their growth during the fiber solidification. Following these results we consider that the elasticity (breaking strain) of the electrospun PLLA scaffolds is controllable by the solvent vapor pressure.

- [1] A. Pathiraja, Gunatillake, R. Adhikari, *European cells and materials* **2003**, 5, 1.
- [2] J. C. Middleton, A. Tipton, *Biomaterials* **2000**, 21, 2335.
- [3] H. Pistner, D. R. Bendix, J. Mühling, J. F. Reuther, *Biomaterials* **1993**, 14, 291.
- [4] M. Vert, P. Christel, F. Chabot, J. Leray, G. W. Hastings, P. Ducheyne, Eds., "Macromolecular Biomaterials", CRC Press, Boca Raton 1984, p. 119.
- [5] K. A. Athanasiou, G. G. Niederauer, A. C. Mauli, *Biomaterials* **1996**, 17, 93.
- [6] S. D. Incardona, L. Fambri, C. Migliaresi, *Materials in medicine* **1996**, 7, 387.
- [7] K. Burg, S. Porter, J. F. Kellam, *Biomaterials* **2000**, 21, 2347.
- [8] L. D. Shea, E. Smiley, J. Bonadio, D. J. Mooney, *Nature biotechnology* **1999**, 17, 551.
- [9] D. H. Reneker, I. Chun, *Nanotechnology* **1996**, 7, 216.
- [10] D. Li, Y. N. Xia, *Advanced Materials* **2004**, 16, 1151.
- [11] D. Reneker, A. Yarin, H. Fong, S. Koombhongse, *J Appl Phys* **2000**, 87, 4531.
- [12] D. Reneker, I. Chun, *Nanotechnology* **1996**, 7, 216.
- [13] R. Jaeger, M. M. Bergshoeff, C. Batlle, H. Schonherr, G. Vancso, *Macromol Symp* **1998**, 50(127), 141.
- [14] Z. M. Huang, Y. Z. Zhang, M. Kotaki, S. Ramakrishna, *Comp Sci Technol* **2003**, 63, 2223.
- [15] S. A. Riboldi, M. Sampaioles, P. Neuenschwander, G. Cossu, S. Mantero, *Biomaterials* **2005**, 26, 4606.
- [16] M.-S. Khil, D.-I. Cha, H.-Y. Kim, I.-S. Kim, N. Bhattarai, *Journal of Biomedical Materials Research. Part B, Applied Biomaterials* **2003**, 67B, 675.
- [17] L. Buttafoco, N. G. Kolkman, A. A. Poot, P. J. Dijkstra, I. Vermes, J. Feijen, *Journal of Controlled Release* **2005**, 101, 322.
- [18] F. Yang, R. Murugan, S. Wang, S. Ramakrishna, *Biomaterials* **2005**, 26, 2603.
- [19] Z. Ma, M. Kotaki, R. Inai, S. Ramakrishna, *Tissue Engineering* **2005**, 11, 101.
- [20] W. Wang, S. Itoh, A. Matsuda, S. Ichinose, K. Shinomiya, Y. Hata, J. Tanaka, *Journal of Biomedical Materials Research Part A* **2008**, 84A, 557.

- [21] B.-M. Min, G. Lee, S. H. Kim, Y. S. Nam, T. S. Lee, W. H. Park, *Biomaterials* **2004**, 25, 1289.
- [22] T. Jarusuwannapoom, W. Hongrojjanawiwat, S. Jitjaicham, L. Wannatong, M. Nithitanakul, C. Pattamaprom, P. Koombhongse, R. Rangkupan, P. Supaphol, *Eur. Polym. J.* **2005**, 41, 409.
- [23] K. H. Lee, H. Y. Kim, Y. M. La, D. R. Lee, N. H. Sung, *J. Polym. Sci., Part B Polym. Phys* **2002**, 40, 2259.
- [24] J. M. Deitzel, J. Kleinmeyer, D. Harris, N. C. B. Tan, *Polymer* **2001**, 42, 261.
- [25] C. Mit-uppatham, M. Nithitanakul, P. Supaphol, *Macromol. Chem. Phys* **2004**, 205, 2327.
- [26] T. Gv. Kooten, J. F. Whitesides, Av. Recum, *J Biomed Mater Res* **1998**, 43, 1.
- [27] N. Patel, R. Padera, G. H. W. Sanders, S. M. Cannizzaro, M. C. Davies, R. Langer, C. J. Roberts, S. J. B. Tendler, P. M. Williams, K. M. Shakesheff, **1998**, 12, 1447
- [28] L. Wannatong, A. Sirivat, P. Supaphol, *Polym. Int* **2004**, 53, 1851.
- [29] S.-H. Tan, R. Inai, M. Kotaki, S. Ramakrishna, *Polymer* **2005**, 46, 6128.
- [30] S. Li, S. McCarthy, *Macromolecules* **1999**, 32, 4454.
- [31] E. N. Ganic, T. G. Hicks, "Engineering Companion McGraw-Hill's", **2002**.
- [32] F. Yoshii, K. Makuuchi, I. Ishigaki, *Journal of Applied Polymer Science* **1986**, 32, 5669.
- [33] H. Ssclji, Y. Ikada, *Polymer* **1995**, 36, 2709.
- [34] S.-C. Wong, A. Baji, S. Leng, *Polymer* **2008**, 49, 4713.
- [35] G. H. Kim, H. Yoon, *Appl. Phys. Lett* **2008**, 93, 023127.